ARTICLE NO. 79-1665R

Waverider Configurations Derived from Inclined Circular and Elliptic Cones

Maurice L. Rasmussen*
University of Oklahoma, Norman, Okla.

Lifting-body waverider configurations, with curved surfaces and known pressure fields and shock-layer structures, are constructed from stream surfaces generated by means of supersonic flows past inclined circular and elliptic cones. The conical flowfields are perturbations of the basic axisymmetric cone flow arising from small angle of attack and small cross-sectional eccentricity. The approximate results are analytic and in the form of hypersonic small-disturbance theory. Formulas are presented that determine how the Mach number, angle of attack, cross-sectional eccentricity, and characteristic cone angle affect the waverider shape, pressure distribution, and shock-layer structure.

Nomenclature

a = tangent of semivertex angle of semiminor axis
b = tangent of semivertex angle of semimajor axis
e = eccentricity factor for elliptic cone, Eq. (2b)
$\bar{g}$ = angle-of-attack shock eccentricity factor
g = elliptic-cone shock eccentricity factor
K_δ = hypersonic similarity parameter $= M_\infty \delta$
M = freestream Mach number
p_0 = pressure for basic circular cone
$\tilde{p}_1$ = perturbation pressure for angle of attack
p_1 = perturbation pressure for cross-sectional eccentricity
r, Θ, ϕ = spherical curvilinear coordinates
s = entropy
u_0, v_0 = radial and polar velocity components associated with basic circular cone
$\tilde{u}_1, \tilde{v}_1, \tilde{w}_1$ = spherical velocity-component perturbations associated with angle of attack
u_1, v_1, w_1 = spherical velocity-component perturbations associated with elliptic cone
V_∞ = freestream velocity
w^* = azimuthal velocity function, Eq. (15)
α = angle of attack
β = shock angle for basic cone
β_w = shock angle for wedge
γ = ratio of specific heats
δ = semivertex angle of basic circular cone, Eq. (4a)
ϵ = perturbation parameter for cross-sectional eccentricity, Eq. (4b)
ξ_0 = density ratio across basic shock $= (\sigma^2 - 1)/\sigma^2$
λ = lip angle of waverider
ρ = density
ϕ_s = streamsurface location on the shock
σ = β/δ, Eq. (6)
Θ_c = polar angle for elliptic cone, Eq. (1) or (3)
Θ_m = mean cone angle, Eq. (2a)
Θ_s = shock angle, Eq. (5)

Presented as Paper 79-1665 at the AIAA Atmospheric Flight Mechanics Conference, Boulder, Colo., Aug. 6-8, 1979; submitted Oct. 19, 1979; revision received April 21, 1980.

Index categories: Supersonic and Hypersonic Flow; LV/M Configurational Design; Spacecraft Configurational and Structural Design.

*Professor, Aerospace, Mechanical, and Nuclear Engineering. Associate Fellow AIAA.

Introduction

THE design of an aircraft for high supersonic flight that achieves desirable aerodynamic behavior and still accommodates such demands as propulsion, structures, materials, and operations is a very challenging task. The requirements of such hypersonic aircraft are discussed by Küchemann[1] and by Küchemann and Weber.[2] When the Mach numbers are sufficiently high that the flow disturbances are intrinsically nonlinear, a treatment of the problem by means of linearized theory is not appropriate. A generalized study of the problem by means of numerical solutions of the nonlinear governing equations of fluid mechanics is very formidable indeed. For this reason the few known exact solutions for flows past elementary geometries are extremely important. These basic exact solutions provide insight and a knowledge of fundamental physical features associated with high-speed flow. In addition, they can also be used as building blocks for flows past more complex geometries.

A basic scheme for deriving exact solutions for three-dimensional lifting bodies by means of simple two-dimensional wedge flows was set forth by Nonweiler.[3] These results were elaborated upon by Venn and Flower,[4] Nardo,[5] and others. The simplest configurations thus derived are called caret wings, or caret waveriders, because of their caret shape. Because these aerodynamic shapes are derived from basic two-dimensional flows, they generally involve flat surfaces and concomitant sharp corners where these surfaces intersect. These sharp corners may be undesirable when factors such as viscous and heating effects are taken into account.

Corresponding to the flat surfaces generated by the basic wedge-shock flow, curved surfaces can be generated by utilization of the stream surfaces associated with the axisymmetric supersonic flow past a circular cone. Such surfaces were devised by Jones[6] and Woods.[7] These constructions generate curved surfaces and curved shocks that are attached to sharp leading edges. The flows for both the cone-generated surfaces and the wedge-generated surfaces can be classified as conical flows.

Besides the axisymmetrical conical flows, there are also conical flows associated with inclined circular cones and with noncircular cones. These flows generate stream surfaces that could be attractive for constructions of lifting bodies with curved surfaces. The analytical description of these flows, as contrasted with a numerical description, generally involves a perturbation analysis of the basic axisymmetric circular-cone flow. A straight-forward perturbation analysis is not uniformly valid in all the variables, but fails in a vortical layer adjacent to the body surface. The pressure and azimuthal

velocity, however, are uniformly valid across the vortical layer.[8-10] This is very important because the azimuthal perturbation velocity is pertinent in determining the stream surfaces of the flowfield, and the pressure is important in determining the relevant forces on the surfaces. Thus the first-order straight forward perturbation expansion, while being suspect at first glance, is thus pertinent in determining the stream surfaces and related forces on waverider configurations generated by the perturbation results. The object of this investigation is to generate various waverider configurations by means of angle-of-attack and cross-sectional eccentricity perturbations of the basic axisymmetric cone flow.

The present study rests heavily on the fact that approximate analytical expressions are available for the perturbed flows past circular[11,12] and elliptic[13,14] cones at small angle of attack. These results allow for an analytical, as opposed to a numerical, investigation to be performed that leads to results that are simple and easily understood. The effects of freestream Mach number, pertinent cone angle, angle of attack, cross-sectional eccentricity, and ratio of specific heats on the shock shape, shock-layer structure, stream-surface shape, and surface conditions can be readily established. Although the results are approximate, they are accurate enough for the parametric and design considerations that are of primary concern here. When the trends and concepts have become clear, more precise and elaborate schemes of analysis can be undertaken for numerical accuracy.[15]

The main concern of this paper is the generation of stream surfaces that can be used as solid surfaces in lifting-body waverider configurations. How the pressure distributions can be obtained will be outlined, but actual lift, drag, and moment results will not be presented here. Such results, and other results of interest such as reported by Squire,[16] will be the subject of further research. At this stage it can be stated that the lift-drag ratios for the waveriders with freestream upper surfaces are significantly higher than the conical bodies from which they are derived.

General Considerations for Conical Flows

Coordinates and Geometry

Consider the perturbation analysis of conical flows past slender elliptic cones at small angles of attack.[13,14] Spherical coordinates in a body-fixed system are shown in Fig. 1. Let $a \equiv \tan\Theta_a$ and $b \equiv \tan\Theta_b$ be the semivertex angles of the semiminor and semimajor axes of the elliptic cone. Then the elliptic cone is described by

$$\tan\Theta_c = (\tan\Theta_m)/\sqrt{1+e\cos 2\phi} \tag{1}$$

where

$$\tan\Theta_m \equiv \sqrt{2}ab/\sqrt{a^2+b^2} = b\sqrt{1-e} = a\sqrt{1+e} = \sqrt{ab}(1-e^2)^{1/4} \tag{2}$$

$$e \equiv (b^2-a^2)/(b^2+a^2)$$

The parameter e is a measure of the eccentricity of the elliptic cone. For small eccentricities Eq. (1) can be expanded in a Fourier series, the first two terms of which are

$$\Theta_c = \delta - \epsilon\cos 2\phi + 0(\epsilon^2) \tag{3}$$

where

$$\delta \equiv \Theta_m + (e^2/32)[3-2\sin^2\Theta_m]\sin 2\Theta_m + 0(e^4) \tag{4}$$

$$\epsilon \equiv (e/4)\{1+(e^2/32)[15-20\sin^2\Theta_m+8\sin^4\Theta_m] + 0(e^4)\}\sin 2\Theta_m$$

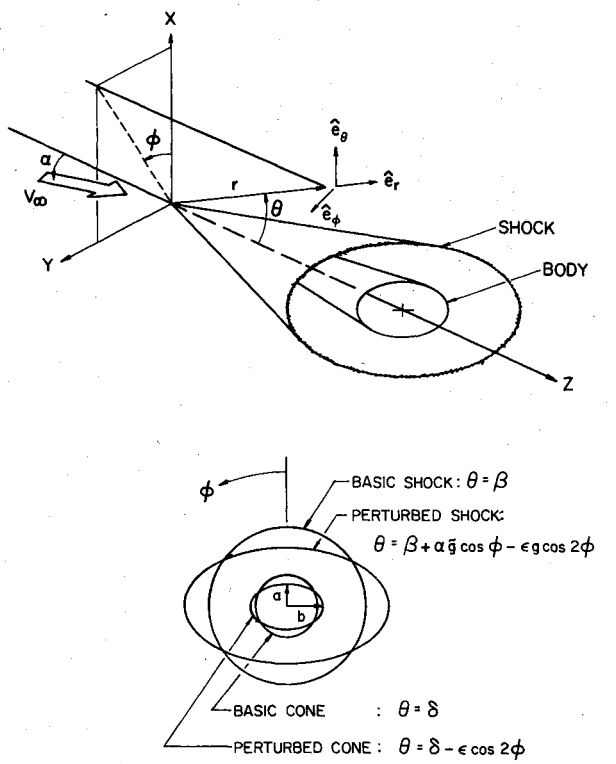

Fig. 1 Cone coordinates and geometry.

The parameter ϵ is a new measure of the eccentricity and is the appropriate small parameter in a perturbation procedure. The parameter δ specifies the semivertex angle of the basic circular cone about which the perturbation expansion is performed.

For small α and ϵ the conical shock wave attached to the elliptic cone has the form[13,14]

$$\Theta_s = \beta + \alpha\tilde{g}\cos\phi - \epsilon g\cos 2\phi \tag{5}$$

where

$$\beta/\delta = [(\gamma+1)/2 + 1/K_\delta^2]^{1/2} \tag{6}$$

and $K_\delta \equiv M_\infty\delta$ is the hypersonic similarity parameter. The parameters $\tilde{g}$ and g are the shock eccentricity factors associated with angle of attack and elliptic cone eccentricity. They are functions of K_δ and are shown in Fig. 2. Analytic expressions are given in the Appendix.

The Shock-Layer Structure

Let u, v, and w denote the r,Θ, and ϕ spherical components of velocity, and let p denote the pressure. Outside the surface vortical layer and the viscous boundary layer, the variables have the following first-order expansions for small α and ϵ:

$$\begin{aligned}
u(\Theta,\phi) &= u_0(\Theta) + \alpha\tilde{u}_1(\Theta)\cos\phi + \epsilon u_1(\Theta)\cos 2\phi \\
v(\Theta,\phi) &= v_0(\Theta) + \alpha\tilde{v}_1(\Theta)\cos\phi + \epsilon v_1(\Theta)\cos 2\phi \\
w(\Theta,\phi) &= \alpha\tilde{w}_1(\Theta)\sin\phi + \epsilon w_1(\Theta)\sin 2\phi \\
p(\Theta,\phi) &= p_0(\Theta) + \alpha\tilde{p}_1(\Theta)\cos\phi + \epsilon p_1(\Theta)\cos 2\phi
\end{aligned} \tag{7}$$

The lowest-order terms in the expansions, with the subscript zero, pertain to the basic-cone solution. The first-order terms with the tilde notation pertain to the angle-of-attack perturbation, and the first-order terms without the tilde notation pertain to the elliptic-cone eccentricity perturbation. The pressure and the azimuthal velocity components, $\tilde{w}_1(\Theta)$ and $w_1(\Theta)$, are uniformly valid across the vortical layer.[9]

To lowest order in α and ϵ, only the azimuthal velocity components $\tilde{w}_1(\Theta)$ and $w_1(\Theta)$ are important in determining

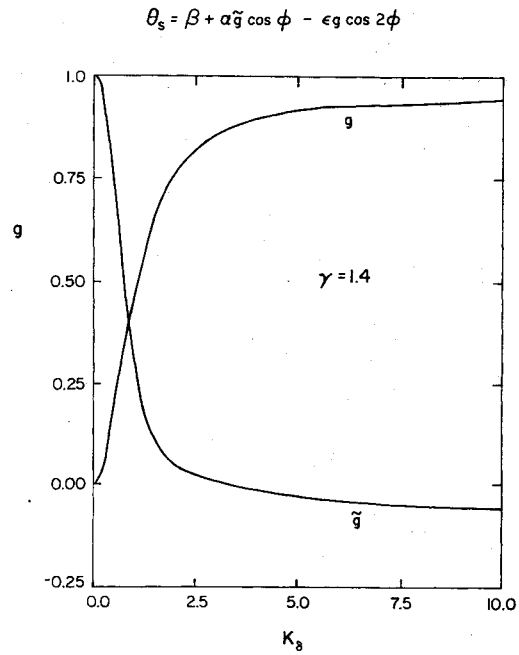

Fig. 2 Shock eccentricity factors.

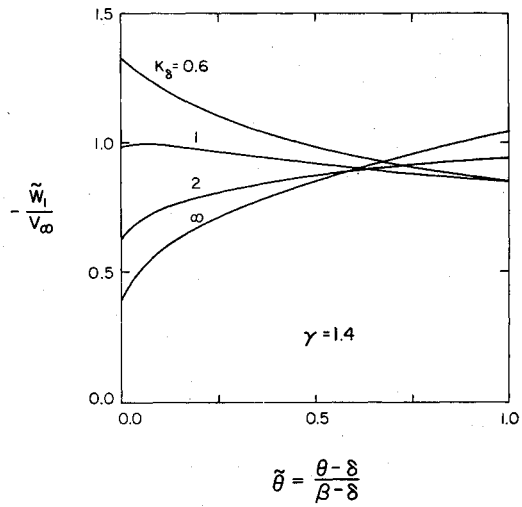

Fig. 3a Angle-of-attack azimuthal velocity perturbation.

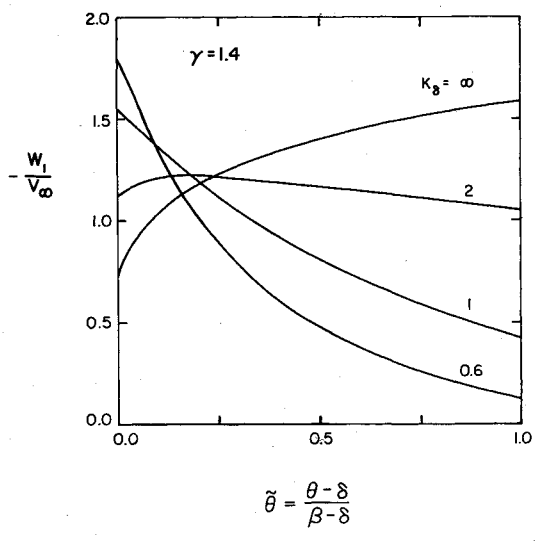

Fig. 3b Cross-sectional eccentricity azimuthal velocity perturbation.

the stream surfaces. The functions $\tilde{w}_1$ and w_1 are plotted in Figs. 3a and b as a function of the normalized coordinate

$$\tilde{\Theta} = (\Theta - \delta)/(\beta - \delta) \tag{8}$$

and the parameter K_δ. At the cone surface, $\tilde{\Theta} = 0$, and at the shock, $\tilde{\Theta} = 1$, correct to within the first-order analysis. All the perturbation variables are summarized in Ref. 17.

Conical Stream Surfaces

The vector equation for a streamline, $V \times \mathbf{ds} = \mathbf{0}$, can be written in spherical coordinates as

$$\frac{dr}{u(\Theta,\phi)} = \frac{r d\Theta}{v(\Theta,\phi)} = \frac{r\sin\Theta d\phi}{w(\Theta,\phi)} \tag{9}$$

The conical stream surfaces are determined by the last two terms of Eq. (9). For small angles and to lowest order, Eq. (9) leads to

$$\frac{d\Theta}{\Theta v_0(\Theta)} = \frac{d\phi}{\alpha\tilde{w}_1(\Theta)\sin\phi + \epsilon w_1(\Theta)\sin 2\phi} \tag{10}$$

To lowest order, only the zeroth-order polar velocity, $v_0(\Theta)$, for the basic cone and the uniformly valid azimuthal perturbation velocities, $\tilde{w}_1(\Theta)$ and $w_1(\Theta)$, enter the analysis. Even though these velocity functions are known, it does not appear possible to obtain an integral of Eq. (10) analytically. In the cases when α or ϵ vanish separately, the variables in Eq. (10) can be separated, and integration can then be obtained at least by quadratures.

The polar velocity, $v_0(\Theta)$, can be approximated accurately for small angles by[11-14,18]

$$v_0(\Theta) = -V_\infty\Theta(1 - \delta^2/\Theta^2) \tag{11}$$

Other formulas for the basic-cone flow and the perturbed flow are summarized in the Appendix.

Approximation for the Stream Surfaces

Preliminary Considerations

It is first useful to rewrite Eq. (10) in the form

$$\frac{\alpha\tilde{w}_1(\Theta) + 2\epsilon w_1(\Theta)}{V_\infty(\Theta^2 - \Theta_c^2)}d\Theta = -\frac{d\phi}{\sin\phi[k_3(\Theta) + k_4(\Theta)\cos\phi]} \tag{12}$$

where without loss in order of accuracy δ in Eq. (11) was replaced by

$$\Theta_c \equiv \delta - \epsilon\cos 2\phi \tag{13}$$

and where

$$k_3(\Theta) \equiv \frac{\alpha\tilde{w}_1(\Theta)}{\alpha\tilde{w}_1(\Theta) + 2\epsilon w_1(\Theta)} \qquad k_4(\Theta) \equiv \frac{2\epsilon w_1(\Theta)}{\alpha\tilde{w}_1(\Theta) + 2\epsilon w_1(\Theta)} \tag{14}$$

When $\epsilon = 0$, that is, the limiting case of a circular cone at angle of attack, then $k_3 = 1$ and $k_4 = 0$ and the variables are separable in Eq. (12), and integration is possible at least by quadratures. When $\alpha = 0$, that is, the limiting case of an elliptic cone aligned with the freestream, then $k_3 = 0$ and $k_4 = 1$, then integration by quadratures is again possible if Θ_c is treated as a constant, which is permissible to the order of accuracy involved in the perturbation analysis. When α and ϵ

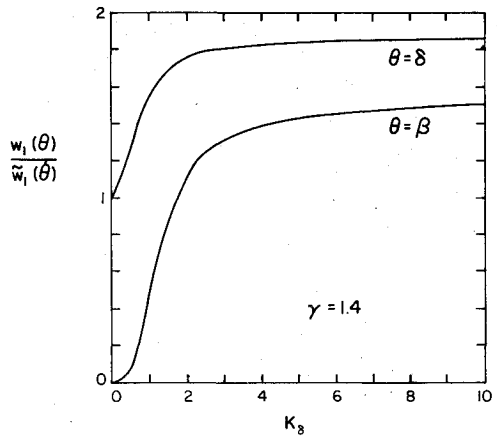

Fig. 4 Azimuthal velocity ratios at shock and body.

are not both zero, Eq. (12) is singular when the combination

$$w^*(\Theta,\phi) \equiv k_3 + k_4 \cos\phi \tag{15}$$

vanishes in the shock layer. The azimuthal location $\phi=\phi_0$ where w^* vanishes is determined by

$$\cos\phi_0 = -\frac{\alpha}{2\epsilon}\frac{\tilde{w}_1(\Theta)}{w_1(\Theta)} \tag{16}$$

which describes a conical surface in the windward side of the shock layer. This surface intersects the body conical surface at the position $\phi_0=\phi_{0c}$ determined by

$$\cos\phi_{0c} = -\frac{\alpha}{2\epsilon}\frac{\tilde{w}_1(\Theta_c)}{w_1(\Theta_c)} \simeq -\frac{\alpha}{2\epsilon}\frac{\tilde{w}_1(\delta)}{w_1(\delta)} \tag{17}$$

The ratio $w_1(\Theta)/\tilde{w}_1(\Theta)$ is shown in Fig. 4 for the limiting values of $\Theta=\Theta_c\simeq\delta$ (body) and $\Theta=\Theta_s\simeq\beta$ (shock). Between the body cone and the surface $w^*=0$ the azimuthal velocity is positive, and it is negative between the $w^*=0$ surface and the shock surface, such as illustrated in Fig. 5a.

It is useful to obtain an approximate integration of Eq. (12) by quadratures by treating k_3 and k_4 as constants. Experience shows that the best values to use for these constants are the values at the body, that is, $k_3\simeq k_3(\delta)$ and $k_4\simeq k_4(\delta)$. For this choice, the body surface conditions are correctly given, which is especially important for the position of the intersection of the windward-leeward dividing stream surface with the body, denoted by ϕ_{0c}.

Although rational approximations for $\tilde{w}_1(\Theta)$ and $w_2(\Theta)$ exist,[12,14] they do not lend themselves to analytical forms for the integrals of Eq. (12). It is useful to use these results, however, for simple approximations valid across the shock layer. Figures 3a and b suggest the following representations for $\tilde{w}_1(\Theta)$ and $w_1(\Theta)$:

$$\tilde{w}_1(\Theta) \simeq \tilde{A} + \Theta_c\tilde{B}/\Theta \tag{18}$$

where

$$\tilde{A} \equiv \frac{\sigma\tilde{w}_1(\beta)-\tilde{w}_1(\delta)}{\sigma-1} \qquad \tilde{B} \equiv \frac{\sigma[\tilde{w}_1(\delta)-\tilde{w}_1(\beta)]}{\sigma-1} \tag{19}$$

and

$$w_1(\Theta) \simeq A + \Theta_c B/\Theta \tag{20}$$

where

$$A \equiv \frac{\sigma w_1(\beta)-w_1(\delta)}{\sigma-1} \qquad B \equiv \frac{\sigma[w_1(\delta)-w_1(\beta)]}{\sigma-1} \tag{21}$$

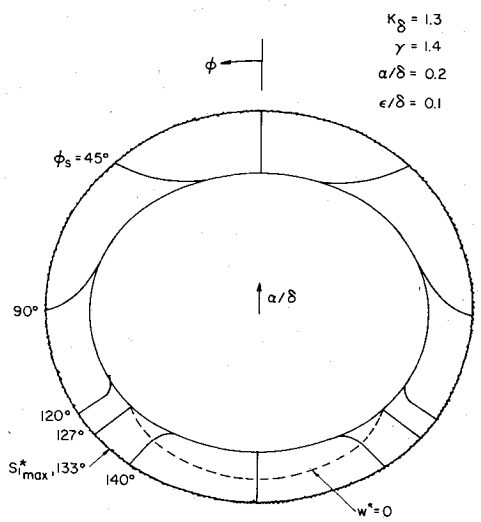

Fig. 5a Stream surfaces for inclined elliptic cone.

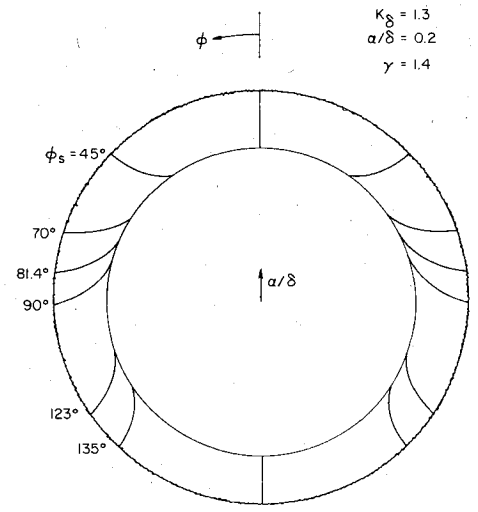

Fig. 5b Stream surfaces for inclined circular cone.

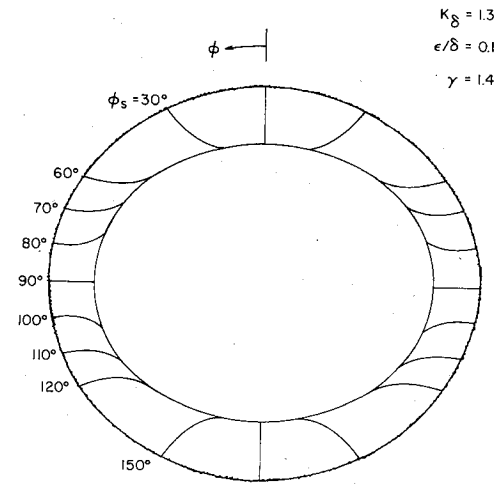

Fig. 5c Stream surfaces for aligned elliptic cone.

and $\sigma\equiv\beta/\delta$ is the basic shock-body angle ratio defined by Eq. (6). These approximations give the correct values at the shock and body surfaces to within first-order accuracy for small α and ϵ. The values of $\tilde{w}_1(\beta)$, $\tilde{w}_1(\delta)$, $w_1(\beta)$, and $w_1(\delta)$ are given in the Appendix as functions of the similarity parameter $K_\delta \equiv M_\infty\delta$.

Conical Stream Surfaces

With the approximate formulas (18) and (19) for the azimuthal velocities and with k_3 and k_4 approximated by the body values, Eq. (12) can be integrated from the shock location $\phi=\phi_s$, and the result written in the form

$$\left[\frac{\Theta-\Theta_c}{\Theta_s^*-\Theta_c^*}\cdot\frac{\Theta_s^*}{\Theta}\right]^{k_1+k_1}\left[\frac{\Theta+\Theta_c}{\Theta_s^*+\Theta_c^*}\cdot\frac{\Theta_s^*}{\Theta}\right]^{k_2+k_2}$$

$$=\left[\frac{\tan(\phi/s)}{\tan(\phi_s/2)}\right]^{k_5}\left[\frac{\tilde{k}_1\csc\phi+k_1\cot\phi}{\tilde{k}_1\csc\phi_s+k_1\cot\phi_s}\right]^{k_6} \tag{22}$$

where

$$\tilde{k}_1\equiv-\frac{1}{2}\frac{\alpha}{\delta}\frac{\tilde{w}_1(\delta)}{V_\infty}\qquad \tilde{k}_2\equiv-\frac{\alpha}{\delta}\frac{(\sigma+1)\tilde{w}_1(\delta)-2\sigma\tilde{w}_1(\beta)}{2(\sigma-1)V_\infty}$$

$$k_1\equiv-\frac{\epsilon}{\delta}\frac{w_1(\delta)}{V_\infty}\qquad k_2\equiv-\frac{\epsilon}{\delta}\frac{(\sigma+1)w_1(\delta)-2\sigma w_1(\beta)}{(\sigma-1)V_\infty}$$

$$k_5\equiv\tilde{k}_1/(\tilde{k}_1-k_1)\qquad k_6\equiv k_1/(\tilde{k}_1-k_1)$$

$$\Theta_c^*\equiv\delta-\epsilon\cos2\phi_s\qquad \Theta_s^*\equiv\beta+\alpha\tilde{g}\cos\phi_s-\epsilon g\cos2\phi_s \tag{23}$$

The right side of Eq. (22) is independent of Θ, whereas the left side depends on both Θ and ϕ, the dependence on ϕ arising from Θ_c. The dependence of the left side on ϕ is weak when ϵ is small, and hence the relation between Θ and ϕ can be calculated with only a few iterations when ϵ is small, and directly when $\epsilon=0$. When ϵ and α vanish separately, expression (22) reduces to the results obtainable from Eq. (12) when k_3 and k_4 are not restricted to their body-surface values. If the conditions are such that $\tilde{k}_1=k_1$, then the appropriate limit must be taken on the right side of Eq. (22), which corresponds to setting $k_3=k_4$ in the original equation (12). Equation (22) can be expected to give a good qualitative description of the stream-surface shapes for small α and ϵ.

Maximum-Entropy Surface

Outside the vortical and viscous boundary layers, the entropy has the expansion

$$s(\Theta,\phi)=s_0(\Theta)+\alpha\tilde{s}_1\cos\phi+\epsilon s_1\cos2\phi \tag{24}$$

where $\tilde{s}_1$ and s_1 are constants associated with the angle-of-attack and eccentricity perturbations. Let

$$s_1^*\equiv\alpha\tilde{s}_1\cos\phi_s+\epsilon s_1\cos2\phi_s \tag{25}$$

denote the entropy perturbation at the shock. It can be shown[11,13,17] that

$$\frac{s_1^*}{c_v}=-\gamma(\gamma-1)\beta(1-\xi_0)^2\frac{V_\infty^2}{a_0^2(\beta)}\left[\alpha(1-\tilde{g})\cos\phi_s+\epsilon g\cos2\phi_s\right] \tag{26}$$

where $\xi_0\equiv\rho_\infty/\rho_0(\beta)$ and $a_0^2(\beta)\equiv\gamma p_0(\beta)/\rho_0(\beta)$. The maximum entropy perturbation at the shock occurs where the derivative with respect to ϕ_s of Eq. (26) vanishes. This occurs where

$$\cos\phi_{sm}=-\alpha(1-\tilde{g})/4\epsilon g \tag{27}$$

If the algebraic value of the right side is less than or equal to minus unity, the maximum occurs at the windward ray, $\phi_s=180$ deg. For the conditions of Fig. 5a ($K_\delta=1.3$, $\gamma=1.4$, $\alpha/\delta=0.2$, $\epsilon/\delta=0.1$), the maximum-entropy stream surface originates at the shock at $\phi_s=133$ deg. This is on the windward side of the dividing stream surface which is located in Fig. 5a at $\phi_s=127$ deg. Thus for the present analysis the maximum-entropy stream surface does not wet the body surface but lies in the windward part of the shock layer. This conical result holds for all values of K_δ. That the body surface and maximum-entropy surface are not necessarily identical is also true for hypersonic blunt-body flows.[19]

Stream-Surface Patterns

Figure 5a shows stream surfaces generated by Eq. (22) for a yawed elliptic cone described by the conditions $K_\delta=1.3$, $\gamma=1.4$, $\alpha/\delta=0.2$, and $\epsilon/\delta=0.1$. The dividing stream surface, which separates the flow that proceeds toward the leeward ray from the flow that proceeds toward the windward ray, occurs at $\phi_s=127$ deg. This dividing surface is a plane surface in this approximation. The actual stream surfaces should appear slightly different near the dividing stream surface and toward the windward ray. In this region the actual stream surfaces have a negative value of azimuthal velocity at the shock and hence should slope towards the leeward direction before curving into the radial direction at the surface $w^*=0$ and then curving further towards the windward ray as shown. Because the details of the azimuthal velocity field have not been taken into account, the dividing stream surface and its intersection with the body surface are not precisely described by the plane surface shown, even though the location of the body intersection is correct. Both the actual slopes and the approximation slopes at the shock are small in the windward region, and hence the description shown in Fig. 5a is qualitatively valid except for the aforementioned discrepancies.

Figure 5b shows the stream surfaces for a yawed circular cone ($K_\delta=1.3$, $\gamma=1.4$, $\alpha/\delta=0.2$, $\epsilon=0$). Except for the leeward ($\phi_s=0$ deg) stream surface and the windward ($\phi_s=180$ deg) stream surface, which lie in the symmetry plane, all the stream surfaces become tangent to the leeward ray on the cone surface. The body surface is the maximum-entropy stream surface.

The stream surfaces for an elliptic cone aligned with the flow are shown in Fig. 5c for the conditions $K_\delta=1.3$, $\gamma=1.4$, $\epsilon/\delta=0.1$, and $\alpha=0$. The body surface is the maximum-entropy stream surface. In this case there are two symmetry planes, aligned with the semimajor and semiminor axes of the ellipse.

Waveriders with Freestream Plane Surfaces

Any stream surface just described can be utilized as a solid surface, but a complementary surface remains to be described in order to fashion a closed aerodynamic body. Here complementary surfaces that are parallel to the freestream are chosen. First, the axis passing through the vertex that is aligned with the freestream is marked out. This axis is inclined by an angle α with the cone axis. Any plane passing through this *freestream axis* is parallel to the freestream. Pairs of these freestream planes that pass through the shock intersection of the conical stream surfaces are now selected and a closed aerodynamic body is thus formed. Thus the upper surfaces are pairs of freestream planes passing through the freestream vertex axis, and the lower surface is a curved stream surface of the conical flowfield. These surfaces intersect at the shock with an angle λ between the surfaces at the intersection line, referred to as the lip angle. There are an infinite number of such aerodynamic configurations, depending on how the freestream planes are selected. These configurations are called waveriders, because the resulting body appears to be riding on the attached shock wave beneath it.

Consider waverider configurations generated from the stream surfaces of the yawed circular cone. Figure 6a shows a configuration with the lip intersection at $\phi_s=90$ deg. The lip angle for this case is $\lambda=8.6$ deg. The freestream surfaces are inclined slightly upward for this case and are described as having positive dihedral. Figure 6b illustrates the con-

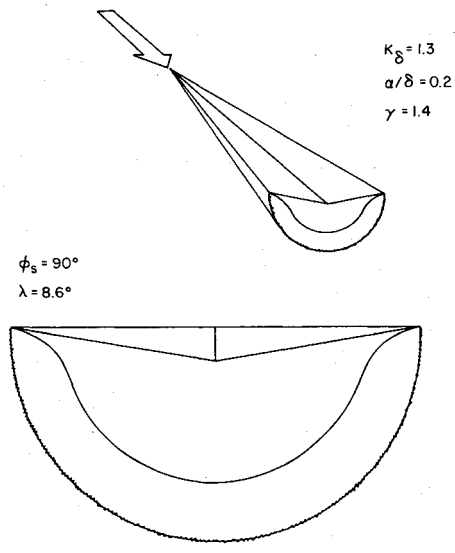

a) Positive dihedral

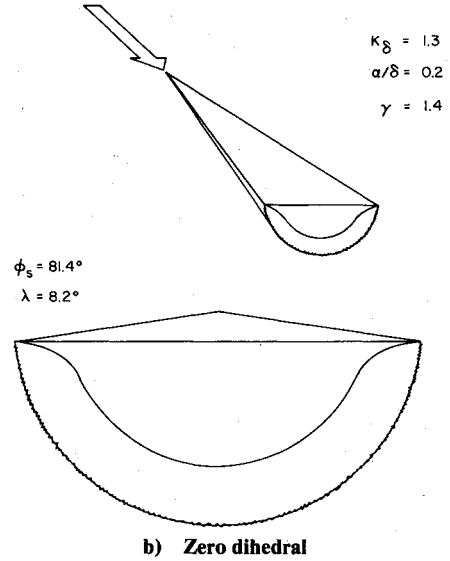

b) Zero dihedral

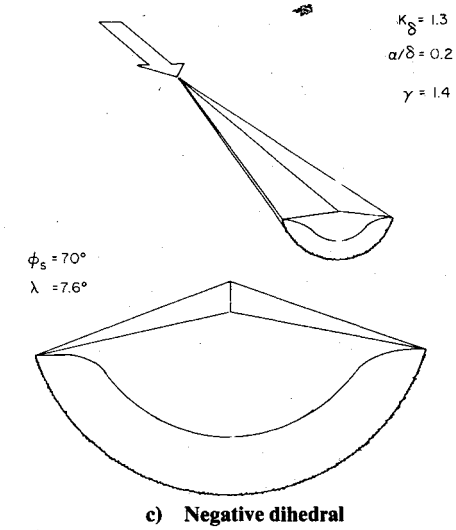

c) Negative dihedral

Fig. 6 Inclined circular-cone waveriders with freestream upper surfaces.

figuration with zero dihedral; the lip intersection is at $\phi_s = 81.4$ deg and the lip angle is $\lambda = 8.2$ deg. The freestream surface is a single flat surface for this case. An example of negative dihedral is shown in Fig. 6c for which $\phi_s = 70$ deg and $\lambda = 7.6$ deg.

Waveriders constructed from the unyawed elliptic cone are shown in Fig. 7. For this case there are no configurations with

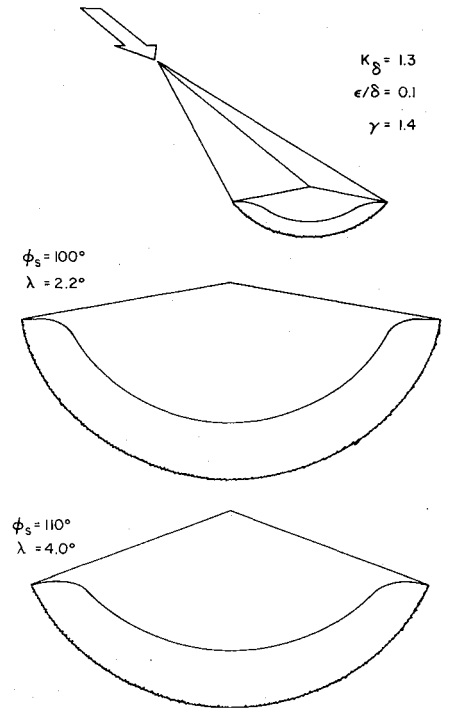

Fig. 7 Elliptic-cone waveriders with freestream upper surfaces.

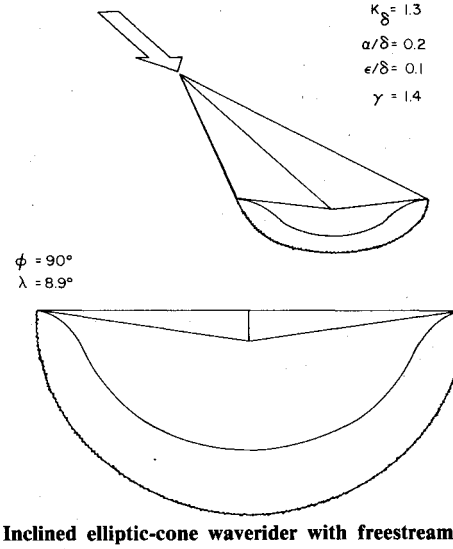

Fig. 8 Inclined elliptic-cone waverider with freestream upper surface: positive dihedral.

positive dihedral. The configurations shown have lip intersections at $\phi_s = 100$ and 110 deg with lip angles of $\lambda = 2.2$ and 4.0 deg. The case of zero dihedral (not shown) corresponds to $\phi_s = 90$ and $\lambda = 0$ deg, and this configuration corresponds to a flat delta wing of zero thickness with an elliptic cone underbody. The configurations derived from the elliptical cone have flatter, more shallow underbodies than the corresponding circular-cone configurations, with sharper lip angles.

Figure 8 shows a configuration derived from the yawed elliptic cone. The lip intersection is at $\phi_s = 90$ deg with a lip angle of $\lambda = 8.9$ deg. This shape has positive dihedral, but zero and negative dihedral configurations are also possible. The pressures on the curved conical surfaces can be computed with formulas given in the Appendix.

Waveriders Constructed with Wedge Shocks

Caret Waveriders

More general waverider configurations can be constructed when the stream surfaces for the classical two-dimensional

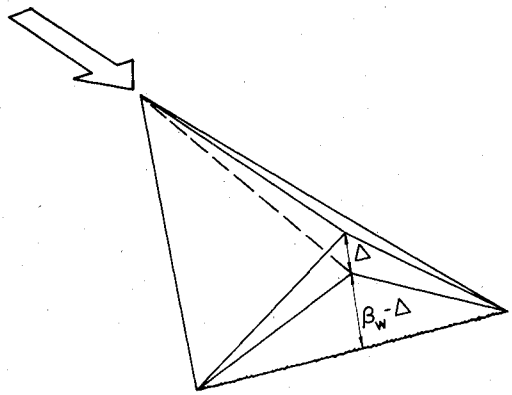

a) Symmetric configuration

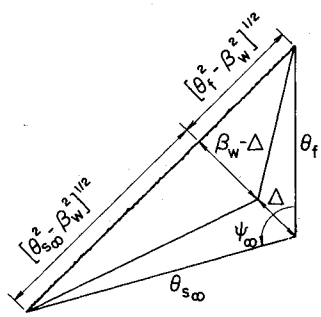

b) Nonsymmetric cross section

Fig. 9 Caret waveriders.

wedge-shock solutions are utilized instead of freestream surfaces. Such stream surfaces by themselves generate what are called caret waveriders. A symmetric caret waverider configuration is shown in Fig. 9a and the cross-section of a nonsymmetric configuration is shown in Fig. 9b. These sketches correspond to small-angle deflections. The freestream flow is deflected by an angle Δ by the plane shock inclined at the angle β_w with the freestream. The plane surfaces denoted $\Theta_{s\infty}$ and Θ_f are parallel to the freestream. When $\Theta_{s\infty}$ and Θ_f are unequal, the caret waverider is nonsymmetric.

The shock angle-deflection angle ratio can be approximated by the hypersonic small disturbance formula[20]

$$\frac{\beta_w}{\Delta} = \frac{\gamma+1}{4} + \left(\frac{\gamma+1}{4} + \frac{1}{M_\infty^2 \Delta^2}\right)^{1/2} \tag{28}$$

which is the counter part of the conical expression (6). The corresponding pressure coefficient for the deflected flow is

$$C_p \equiv 2(p-p_\infty)/\rho_\infty V_\infty^2 = 2\Delta^2(\beta_w/\Delta) \tag{29}$$

Waverider configurations utilizing flat caret waverider surfaces for the upper surfaces complementary to the curved cone-derived surfaces are described in Ref. 17.

Conical Waveriders with Vertical Fins

Now consider a non-symmetric caret waverider such as shown in Fig. 9b. It is desired to fit a pair of such configurations onto the freestream surfaces of our previously devised waveriders in Figs. 6-8. The surface denoted by $\Theta_{s\infty}$ should fit onto the freestream surface from the cone freestream axis to the lip intersection at the shock, both on the left and the right of the freestream axis. The surface denoted by the vertical vertex angle Θ_f will be the center plane of a vertical fin. The magnitude of Θ_f depends on the angle ψ_∞ and the deflection angle Δ.

From geometrical considerations shown in Fig. 9b, the relation

$$\Theta_{s\infty}/\Theta_f = \cos\psi_\infty + \sin\psi_\infty [(\Theta_{s\infty}/\beta_w)^2 - 1]^{1/2} \tag{30}$$

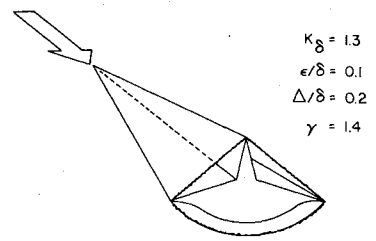

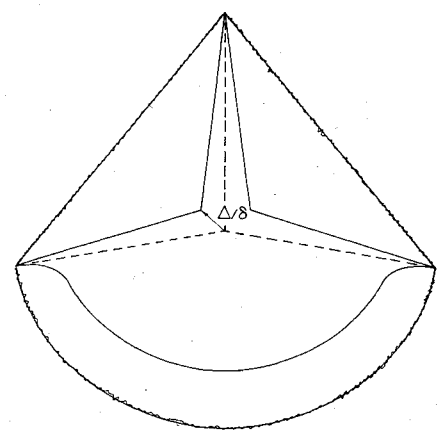

a) Fin starting at vertex

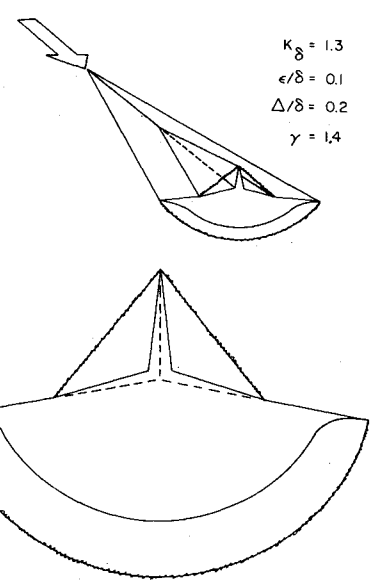

b) Fin starting at half length

Fig. 10 Elliptic-cone waveriders with vertical fins.

can be established. When β_w is determined by Eq. (28), Eq. (30) constitutes a relation for Θ_f/δ as a function of $\Theta_{s\infty}/\delta$, ψ_∞, Δ/δ, K_δ, and γ.

Consider now the case of the unyawed elliptic cone waveriders shown in Fig. 7. In this case $\Theta_{s\infty} = \Theta_2^* \equiv \beta - \epsilon g \cos 2\phi_s$ and $\psi_\infty = \phi_s$. Now for $K_\delta = 1.3$, $\gamma = 1.4$, $\epsilon/\delta = 0.1$ and $\phi_s = 100$ deg, and for Δ/δ values of 0, 0.1, and 0.2, respectively, the values of Θ_f/δ are 1.06, 1.21, and 1.40. The case $\Delta = 0$ corresponds to the limiting Mach wave for β_w, and thus the minimum value of Θ_f.

Since the freestream surfaces of the caret waverider and elliptic-cone waverider are coplanar, the vertical fin can start at the cone vertex or at some position behind the vertex. The configuration for which the fin starts at the vertex is shown in Fig. 10a for $\Delta/\delta = 0.2$. In this case the fin shock is attached to the conical lip. The case where the fin begins halfway back on the elliptic-cone undersurface is shown in Fig. 10b for $\Delta/\delta = 0.2$. These vertical-fin configurations are of interest for the implementation of vertical control surfaces.

Concluding Remarks

By means of stream surfaces obtained from angle-of-attack and cross-sectional eccentricity perturbations of the basic supersonic axisymmetric flow past a circular cone, aerodynamic lifting-body configurations have been derived. The emphasis has been on systematic parametric study on the various configurations that can be obtained. The configurations have attached shocks on sharp leading edges and thus can be described as conical waveriders. Utilization of wedge-shock caret-waverider results leads to a combination of configurations and to vertical-fin control surfaces.

The analysis has proceeded within the framework of hypersonic small-disturbance theory, and approximate analytic formulas have been derived that apply over a wide range of conditions. Although pressure distributions have not been calculated, the pertinent formulas have been recorded in the Appendix. Further calculations by interested investigators can be performed readily.

The lifting-body configurations that have been presented appear attractive in terms of high lift-drag ratio requirements. Further work is required to account for other aerodynamic factors. Some of these are 1) lift, drag, and moment characteristics, 2) boundary-layer growth and related viscous effects, 3) off-design effects, 4) details of flaps and other control surfaces, 5) unsteady flow and dynamic forces and moments, 6) blunted edges and noses, and 7) experimental results.

Appendix: Formulas for the Inclined Elliptic Cone Flow Perturbations

The following formulas for the shock shape, azimuthal velocity perturbation, and pressure perturbation are recorded here.[11-14,17] The shock eccentricity factors are given by

$$\tilde{g}=\frac{3+2\sigma^2\left[3-\dfrac{4(1+\sigma^2)}{\gamma+1}\right]-\dfrac{\ell n[\sigma+\sqrt{\sigma^2-1}]}{\sigma\sqrt{\sigma^2-1}}}{5-2(1+\sigma^2)\left[1+\dfrac{4\sigma^2}{\gamma+1}\right]-\dfrac{\ell n[\sigma+\sqrt{\sigma^2-1}]}{\sigma\sqrt{\sigma^2-1}}}$$

$$g=6\sigma^3\left[\frac{3\cos^{-1}(1/\sigma)}{\sqrt{\sigma^2-1}}+\frac{6}{\gamma+1}(\sigma^6+\sigma^2)+3\sigma^4-\sigma^2-5\right]^{-1}$$

where $\sigma\equiv\beta/\delta$ is given by Eq. (6). The azimuthal velocities at the shock and body surface are given by

$$\tilde{w}_1(\beta)=-[1-\tilde{g}(1-\xi_0)]V_\infty \qquad w_1(\beta)=-2g(1-\xi_0)V_\infty$$

$$\tilde{w}_1(\delta)=-\left[-(1+\tilde{g})+\frac{1-\tilde{g}}{2\sigma^2}\left\{\frac{8\sigma^4}{\gamma+1}-1-\frac{\ell n[\sigma+\sqrt{\sigma^2-1}]}{\sigma\sqrt{\sigma^2-1}}\right\}\right]V_\infty$$

$$w_1(\delta)=-g\left[\sigma-\frac{1}{3\sigma}+\frac{1}{3\sigma^3}+\frac{2}{\gamma+1}\left(\sigma^3-\frac{1}{\sigma}\right)-\frac{\cos^{-1}(1/\sigma)}{\sigma\sqrt{\sigma^2-1}}\right]V_\infty$$

where

$$\xi_0\equiv\rho_\infty/\rho_0(\beta)\simeq(\sigma^2-1)/\sigma^2$$

The pressure in the shock layer is given by Eq. (7d). The pressure for the basic cone solution is given by[17,18]

$$\frac{p_0(\Theta)}{p_\infty}=1+\frac{\gamma K_\delta^2}{2}\left[1+\frac{\sigma^2}{\sigma^2-1}\left\{1-\frac{\delta^2}{\Theta^2}+\ell n\left(\frac{\beta^2}{\Theta^2}\right)\right\}\right]$$

The pressure perturbations $\tilde{p}_1(\Theta)$ and $p_1(\Theta)$ have explicit relations but they are very lengthy and complicated.[12,14] It is useful alternatively to use a linear variation across the shock layer in the forms

$$\tilde{p}_1(\Theta)=\tilde{p}_1(\delta)+\frac{\Theta-\delta}{\beta-\delta}\left[\tilde{p}_1(\beta)-\tilde{p}_1(\delta)\right]$$

$$p_1(\Theta)=p_1(\delta)+\frac{\Theta-\delta}{\beta-\delta}\left[p_1(\beta)-p_1(\delta)\right]$$

The shock and body values are given by[12,14,17]

$$\tilde{p}_1(\beta)=-\rho_\infty V_\infty^2\beta\left[\frac{4(1-\tilde{g})}{\gamma+1}-\frac{\tilde{g}}{\sigma^2}\right]$$

$$p_1(\beta)=-\rho_\infty V_\infty^2 g\beta\left[\frac{4}{\gamma+1}+\frac{1}{\sigma^2}\right]$$

$$\tilde{p}_1(\delta)\simeq\frac{\gamma\delta V_\infty p_0(\delta)\tilde{w}_1(\delta)}{a_0^2(\delta)}$$

$$p_1(\delta)\simeq\frac{\gamma\delta V_\infty p_0(\delta)w_1(\delta)}{2a_0^2(\delta)}$$

where

$$\frac{a_0^2(\delta)}{a_\infty^2}=1+\frac{\gamma-1}{2}K_\delta^2\left[1+\ell n\sigma^2\right] \qquad a_\infty^2\equiv\frac{\gamma p_\infty}{\rho_\infty}$$

Acknowledgments

This work was sponsored by the Air Force Office of Scientific Research under AFOSR Grant 77-3468 and by the Air Force Armament Laboratory under Contract FO 8635-79-C-0017. The author is grateful for discussions with Martin Jischke and Don Daniel.

References

[1] Küchemann, D., "Hypersonic Aircraft and Their Aerodynamic Problems," *Progress in Aeronautical Sciences,* Vol. 6, edited by D. Küchemann and L.H.G. Stern, Pergamon Press, London, 1965, p. 271.

[2] Küchemann, D. and Weber, J., "An Analysis of Some Performance Aspects of Various Types of Aircraft Designed to Fly Over Different Ranges at Different Speeds," *Progress in Aeronautical Sciences,* Vol. 9, edited by D. Küchemann et al., Pergamon Press, London, 1968, p. 329.

[3] Nonweiler, T.R.F., "Delta Wings of Shape Amenable to Exact Shock-Wave Theory," *Journal of the Royal Aeronautics Society,* Vol. 67, 1963, p. 39.

[4] Venn, J. and Flower, J.W., "Shock Patterns for Simple Caret Wings," *Journal of the Royal Aeronautics Society,* Vol. 74, 1970, pp. 339-348.

[5] Nardo, C.T., "Aerodynamic Characteristics of Two-Dimensional Waverider Configurations," *AIAA Journal,* Vol. 10, Sept. 1972, p. 1258.

[6] Jones, J.G., "A Method for Designing Lifting Configurations for High Supersonic Speeds Using the Flow Fields of Non-Lifting Cones," Royal Aeronautical Establishment Rept. No. Aero 2674, A.R.C. 24846, 1963.

[7] Woods, B.A., "The Construction of a Compression Surface Based on an Axisymmetrical Conical Flow Field," Royal Aeronautical Establishment Tech. Note No. Aero 2900, A.R.C. 25087, 1963.

[8] Cheng, H.K., "Hypersonic Flows Past a Yawed Circular Cone and Other Pointed Bodies," *Journal of Fluid Mechanics,* Vol. 12, 1962, pp. 169-191.

[9] Munson, A.G., "The Vortical Layer on an Inclined Cone," *Journal of Fluid Mechanics,* Vol. 20, 1964, pp. 625-643.

[10] Melnik, R.E., "Vortical Singularities in Conical Flow," *AIAA Journal,* Vol. 5, April 1967, pp. 631-637.

[11] Doty, R.T., "Hypersonic Flow Past an Inclined Cone," M.S. Thesis, Aerospace, Mechanical, and Nuclear Engineering, University of Oklahoma, 1972.

[12] Doty, R.T. and Rasmussen, M.L., "Approximation for Hypersonic Flow Past an Inclined Cone," *AIAA Journal,* Vol. 11, Sept. 1973, pp. 1310-1315.

[13] Lee, H.M. and Rasmussen, M.L., "Hypersonic Flow Past a Slender Elliptic Cone," University of Oklahoma, School of Aerospace, Mechanical, and Nuclear Engineering, Research Report No. OU-AMNE-78-2, 1978.

[14] Rasmussen, M.L. and Lee, H.M., "Approximation for Hypersonic Flow Past a Slender Elliptic Cone," AIAA Paper 79-0364, AIAA 17th Aerospace Sciences Meeting, New Orleans, Jan. 1979.

[15] Klunker, E.B., South, J.C., and Davis, R.M., "Calculation of Nonlinear Conical Flows by the Method of Lines," NASA TR R-374, Oct. 1971.

[16] Squire, L.C., "The Aerodynamics of Lifting Bodies at High Supersonic Speeds," *Journal of the Royal Aeronautics Society,* Vol. 75, 1971, p. 18.

[17] Rasmussen, M.L., "Lifting Bodies Derived from Supersonic Flows Past Inclined Circular and Elliptic Cones," University of Oklahoma, School of Aerospace, Mechanical, and Nuclear Engineering, Research Report No. OU-AMNE-78-11, 1978.

[18] Rasmussen, M.L., "On Hypersonic Flow Past an Unyawed Cone," *AIAA Journal,* Vol. 5, Aug. 1967, pp. 1495-1497.

[19] Hayes, W.D. and Probstein, R.F., *Hypersonic Flow Theory, Vol. I, Inviscid Flows,* 2nd Ed., Academic Press, New York, 1966.

[20] Linnell, R.D., "Two-Dimensional Airfoils in Hypersonic Flows," *Journal of Aeronautical Sciences,* Vol. 16, 1949, pp. 22-30.